Mechanism of IRK1 Channel Block by Intracellular Polyamines

Donglin Guo and Zhe Lu

From the Department of Physiology, University of Pennsylvania, Philadelphia, Pennsylvania 19104

abstract Intracellular polyamines inhibit the strongly rectifying IRK1 potassium channel by a mechanism different from that of a typical ionic pore blocker such as tetraethylammonium. As in other K^+ channels, in the presence of intracellular TEA, the IRK1 channel current decreases with increasing membrane voltage and eventually approaches zero. However, in the presence of intracellular polyamines, the channel current varies with membrane voltage in a complex manner: when membrane voltage is increased, the current decreases in two phases separated by a hump. Furthermore, contrary to the expectation for a nonpermeant ionic pore blocker, a significant residual IRK1 current persists at very positive membrane voltages; the amplitude of the residual current decreases with increasing polyamine concentration. This complex blocking behavior of polyamines can be accounted for by a minimal model whereby intracellular polyamines inhibit the IRK1 channel by inducing two blocked channel states. In each of the blocked states, a polyamine is bound with characteristic affinity and probability of traversing the pore. The proposal that polyamines traverse the pore at finite rates is supported by the observation that philanthotoxin-343 (spermine with a bulky chemical group attached to one end) acts as a nonpermeant ionic blocker in the IRK1 channel.

key words: inward-rectifier K^+ channel • ion permeation • protonation • polyamine• diamine

INTRODUCTION

Inward-rectifier K^+ channels are blocked by intracellular Mg^{2+} and polyamines (Vandenberg, 1987; Matsuda et al., 1987; Logothetis et al., 1987; Horie et al., 1987; Lopatin et al., 1994; Ficker et al., 1994; Fakler et al., 1995). This block depends strongly on membrane voltage, causing the channel to conduct in an inwardly rectifying manner, enabling the inward-rectifier K^+ channels to accomplish various important biological tasks (Hille, 1992). The voltage dependence of channel block is not exclusively an intrinsic property of the blocking ion because it also depends strongly on the nature and concentration of permeant ions present in the extracellular solution (Oliver et al., 1998; Spassova and Lu, 1998, 1999). Quantitative analyses show that the voltage dependence of channel block results at least in part from the concomitant movement of permeant ions (energetically coupled to the blocking ions) in the transmembrane electrical field (Spassova and Lu, 1998, 1999).

Previous studies of polyamine block of strongly rectifying inward-rectifier K^+ channels have revealed complex phenomena. For example, the relation between the extent of channel block and membrane voltage exhibits a shallower phase and a steep phase, and thus requires an equation with two Boltzmann terms (Lopatin et al., 1995). The extent of channel block as a function of polyamine concentration also exhibits two phases (Yang et al., 1995), requiring an equation with two hyperbolic terms. It has, therefore, been suggested that more than one polyamine molecule can bind to the pore (Lopatin et al., 1995) and may be required for complete block of the channel (Yang et al., 1995; Lu et al., 1999). In the present study, we investigated the mechanism underlying the complex blocking behavior of polyamines in the strongly rectifying IRK1 channel.

Address correspondence to Dr. Zhe Lu, University of Pennsylvania, Department of Physiology, D302A Richard Building, 3700 Hamilton Walk, Philadelphia, PA 19104. Fax: 215-573-1940; E-mail: zhelu@mail.med.upenn.edu

METHODS

Molecular Biology and Oocyte Preparation

IRK1 (Kir2.1) cDNA cloned into the pcDNA1/AMP plasmid (Invitrogen Corp.) was kindly provided by Dr. Lily Y. Jan (Kubo et al., 1993). RNA was synthesized using T7 polymerase (Promega Corp.) from Not1-linearized IRK1 cDNA. Oocytes harvested from *Xenopus laevis* (Xenopus One) were incubated in a solution containing (mM): 82.5 NaCl, 2.5 KCl, 1.0 $MgCl_2$, 5.0 HEPES, pH 7.6, and 2–4 mg/ml collagenase. The oocyte preparation was agitated using a platform shaker (80 rpm) for 60–90 min. It was then rinsed thoroughly with and stored in a solution containing (mM): 96 NaCl, 2.5 KCl, 1.8 $CaCl_2$, 1.0 $MgCl_2$, 5 HEPES, pH 7.6, and 50 μg/ml gentamicin. Defolliculated oocytes were selected and injected with RNA at least 2 and 16 h, respectively, after collagenase treatment. All oocytes were stored in an incubator at 18°C.

Patch Recording and Data Analysis

IRK1 currents were recorded in the inside-out configuration from the membrane of *Xenopus* oocytes (injected with IRK1 cRNA) with an Axopatch 200B amplifier (Axon Instruments, Inc.). The recorded signal was filtered at 1 kHz and sampled at 5 kHz using an analogue-to-digital converter (DigiData 1200; Axon Instruments, Inc.) interfaced with a personal computer. pClamp6 software (Axon Instruments, Inc.) was used to control the amplifier and acquire the data. During the current recording, the voltage across the membrane patch was first hyperpolarized from the 0 mV holding potential to −100 mV for 50 ms (to relieve channel block by the tested intracellular blocker), and then stepped

 J. Gen. Physiol. © The Rockefeller University Press • 0022-1295/2000/06/799/15 $5.00
Volume 115 June 2000 799–813
http://www.jgp.org/cgi/content/full/115/6/799

to a test voltage between −100 and +100 mV, in 5- or 10-mV increments, for 0.3–1 s. Background leak current correction was carried out as previously described (Lu and MacKinnon, 1994; Spassova and Lu, 1998). All curve fittings were carried out using Origin software version 5 (Microcal Software, Inc.).

Recording Solutions

Pipette solution contained (mM): 100 KCl, 0.3 $CaCl_2$, 1.0 $MgCl_2$, and 10 HEPES, pH 7.6. The bath solutions contained (mM): 90 KCl, 5 K_2EDTA, 10 HEPES, pH 7.6 or 6.6, as specified. The bath solutions containing diamines, polyamines, and philanthotoxin-343 (PhTx)[1] were prepared daily.

RESULTS

Channel Block by Intracellular Tetraethylammonium

Tetraethylammonium and all other intracellular IRK1 channel blockers that we studied block the channel in a voltage-dependent manner. To examine the IRK1 current at various membrane voltages, we used a voltage-pulse protocol rather than a ramp, because the current through the IRK1 channel does not instantaneously reach a steady state after a change in membrane voltage (Fig. 1 A). To quantify channel block by a given blocker, we analyzed its effect only on the steady state current. Although the nature of the time-dependent current decline after a step to positive membrane voltages is unknown, intrinsic gating has been suggested as the cause because the current decline persists even after the intracellular side of the membrane patch is exhaustively perfused with recording solution nominally devoid of blocking ions (Aleksandrov et al., 1996; Shieh et al., 1996). Fig. 1 B shows both the "instantaneous" and the "steady state" I-V curves recorded 2 and 300 ms, respectively, after the voltage step. The instantaneous I-V curve exhibits slight inward rectification, while the steady state I-V curve shows stronger rectification. The ratio of the two I-V curves in Fig. 1 B is plotted against membrane voltage in C. The valence factor Z*, which quantifies the voltage dependence of the current decline, is 0.55 ± 0.01 (mean ± SEM), much smaller than those of high-affinity polyamines such as spermidine and spermine. This finding argues that the current decline results from causes other than incomplete removal of high-affinity polyamines.

For the purpose of comparison, we first examined channel block by the classic intracellular ionic pore blocker TEA (Armstrong and Binstock, 1965). Fig. 2 A shows the IRK1 currents recorded without and with various concentrations of intracellular TEA under symmetric K^+ conditions. The membrane was first hyperpolarized to −100 mV for 50 ms, and then depolarized for 300 ms to a test membrane voltage ranging from −100 to +100 mV in 10-mV increments. Outward currents in the presence of intracellular TEA became progressively smaller with membrane depolarization. Consequently,

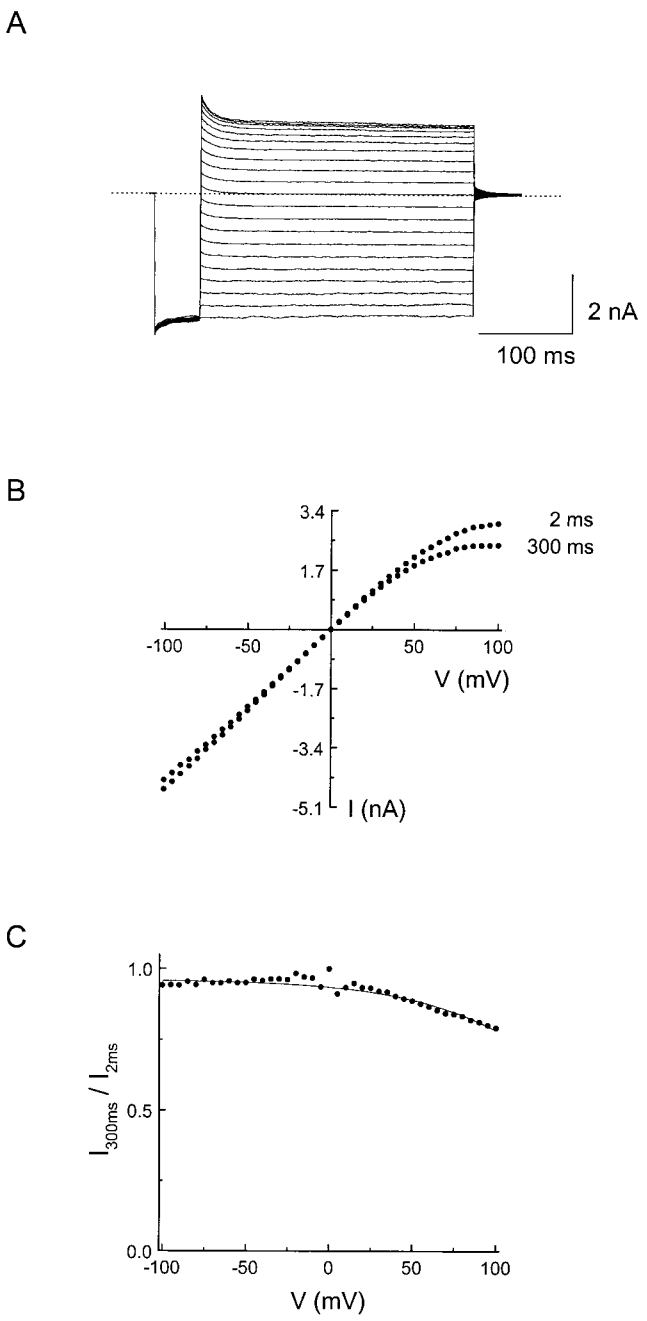

Figure 1. Current–voltage relationship of the IRK1 channel. (A) A family of current traces recorded from an inside-out patch at membrane voltages from −100 to +100 mV in 5-mV increments. However, for clarity, we plotted only the current traces recorded at 10-mV intervals. The recording was made without adding any tested blocking ions in the intracellular solution. (B) The I-V curves of the channel obtained 2 and 300 ms after the start of the voltage step. (C) The ratio of the currents in B is plotted against membrane voltage. The curve superimposed on the data is the fit of equation $I_{300\ ms}/I_{2\ ms} = 1/(1 + K^*e^{Z^*FVm/RT})$, which corresponds to a model where increasing membrane voltage increases the probability of a channel (Ch) entering a nonconducting state (Ch*). The equilibrium constant K^* is defined as the ratio of the fractions of Ch* and Ch, while Z^* is the apparent valence for the transition Ch ↔ Ch*. From the fit, we obtain $K^* = 0.03 \pm 0.01$ and $Z^* = 0.55 \pm 0.01$ (mean ± SEM, $n = 6$).

[1]*Abbreviations used in this paper:* CNG channel, cyclic nucleotide–gated channel; PhTx, philanthotoxin-343.

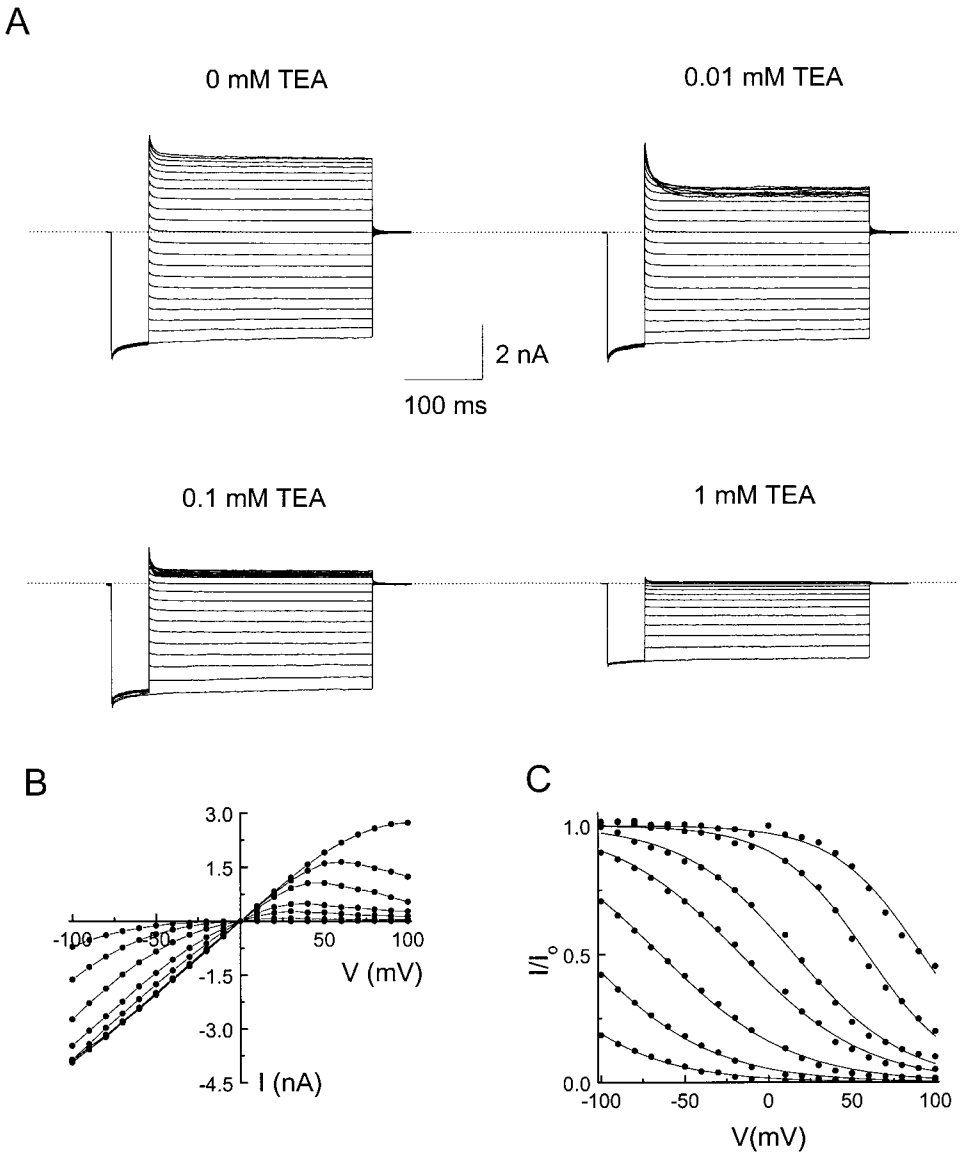

Figure 2. Block of the IRK1 channel by intracellular TEA. (A) Current traces recorded in the absence or presence of various concentrations of TEA. The holding potential was zero. For each experiment, the membrane voltage was first hyperpolarized to −100 mV for 50 ms, and then stepped to various test voltages from −100 to +100 mV, in 10-mV increments, for 300 ms. The dashed lines identify the zero current level. (B) Steady state I-V curves in the absence or presence of TEA at concentrations of 10, 30, 100, and 300 μM, and 1, 3, and 10 mM. The current values were determined at the end of each 300-ms voltage pulse. (C) The fractions of current not blocked by TEA at the seven concentrations in B are plotted as a function of membrane voltage. The curves superimposed on the data are fits of the Woodhull equation, $I/I_o = 1/(1 + [\text{TEA}]/K_d e^{-ZFV/RT})$ (Woodhull, 1973), with K_d = 0.20 ± 0.01 mM and Z = 0.85 ± 0.01 (mean ± SEM, n = 5).

the I-V curves (Fig. 2 B) at positive membrane voltages display significant downward curvature in the presence of TEA. In Fig. 2 C, we plotted the fractions of current not blocked by various concentrations of TEA as a function of membrane voltage. The curves superimposed on the data are fits of the Woodhull equation (a variation of the Boltzmann equation) (Woodhull, 1973). As expected for an ionic pore blocker, the extent of IRK1 channel block by intracellular TEA progressively increases as membrane voltage is made more positive.

Channel Block by Intracellular Putrescine

Fig. 3 A shows current traces recorded in the absence or presence of various concentrations of intracellular putrescine. The recordings were carried out between −100 and +100 mV in 5-mV increments, but, for clarity, we plotted only the current traces recorded at 10-mV intervals. Fig. 3 B plots the I-V curves in the absence and presence of the three concentrations of putrescine. Unlike that in the presence of TEA (compare Fig. 2 B), the IRK1 channel current in the presence of putrescine, after reaching a peak at some positive voltages, did not continue to decline towards zero in the manner expected for a typical ionic pore blocker. Rather, a significant current persists at very positive membrane voltages. The amplitude of the residual current is smaller at higher putrescine concentrations. In Fig. 3 C, we plotted the fractions of unblocked current as a function of membrane voltage. Contrary to the expectation for voltage-dependent block by a typical ionic pore blocker, the extent of channel block for a given putrescine concentration does not follow the Woodhull equation, but approaches a nonzero level at positive membrane voltages. Putrescine clearly does not simply act as a typical ionic pore blocker.

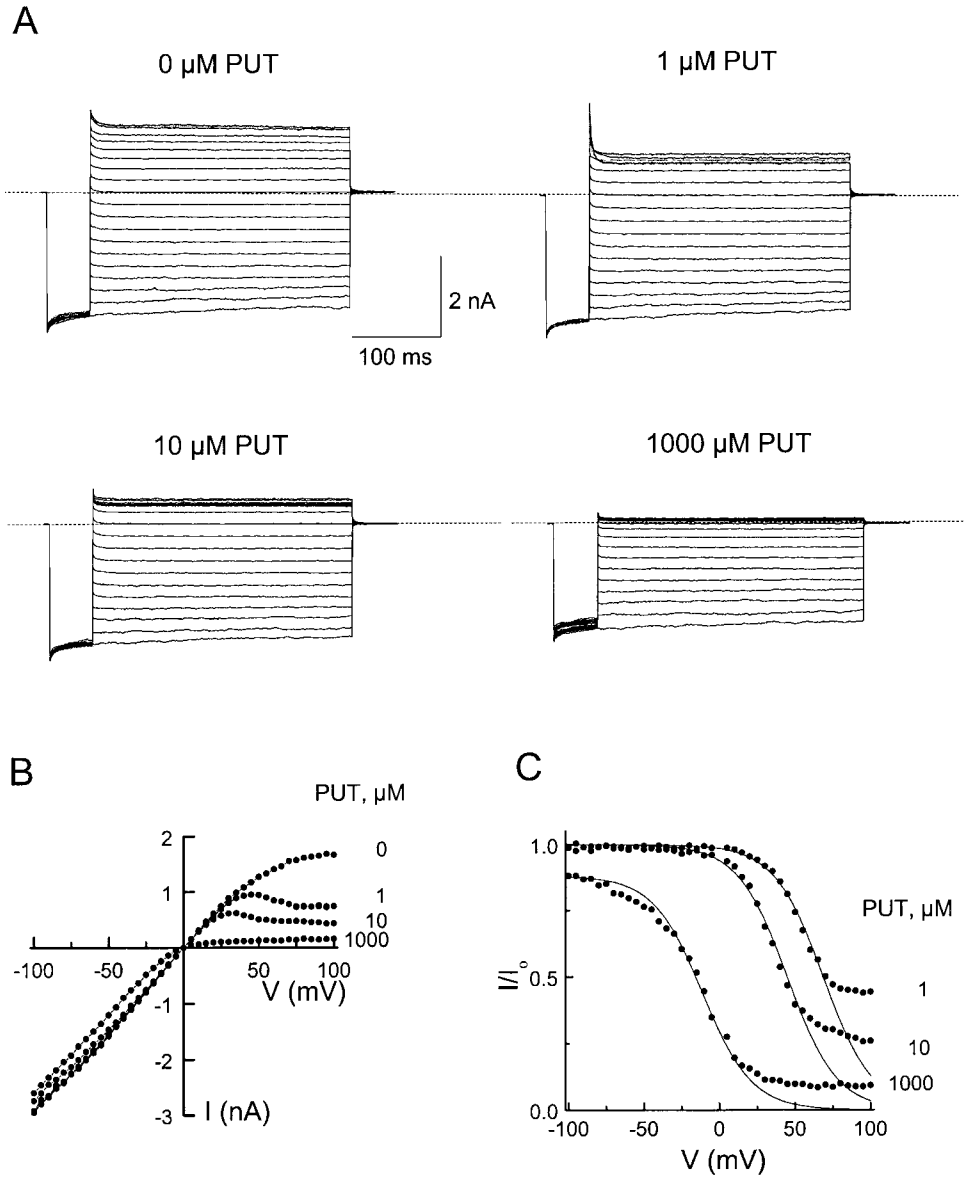

Figure 3. Channel block by intracellular putrescine. (A) Current traces recorded in the absence or presence of various concentrations of putrescine. For each experiment, the membrane voltage was first hyperpolarized to −100 mV for 50 ms, and then stepped to various test voltages from −100 to +100 mV in 5-mV increments for 300 ms. However, for clarity, we only plotted the current traces recorded at 10-mV intervals. (B) I-V curves in the absence or presence of various concentrations of putrescine. (C) The fractions of current not blocked by putrescine are plotted against membrane voltage. The curves were drawn according to the Woodhull equation (Fig. 2).

Channel Block by Intracellular Diamines

To better understand block of the IRK1 channel by putrescine (a primary diamine) described here, we systematically tested a series of primary diamines of varying methylene chain length. Fig. 4 shows the current traces of the IRK1 channel between −100 and +100 mV, recorded in the absence and presence of nine diamines containing from 2 to 10 methylene groups (DM_{C2} through DM_{C10}; putrescine is DM_{C4}). Fig. 5 shows I-V curves obtained without and with the nine diamines at various concentrations including those of Fig 4. Except for DM_{C2}, which blocked the channel slightly more effectively than DM_{C3}, blocking efficacy generally increased with methylene chain length. The effect of each diamine on the I-V curves is qualitatively similar to that of putrescine (DM_{C4}). However, the currents appear to reach a nonzero "plateau" at progressively lower membrane voltages as the methylene chain length increases. In Fig. 6, we plotted the fractions of unblocked current in the presence of the various diamines as a function of membrane voltage. As in the case of putrescine (DM_{C4}), the extent of channel block by each of the diamines tends to a nonzero level at positive membrane voltages, a behavior reminiscent of block of the retinal cGMP-gated (CNG) channel by certain diamines (e.g., DM_{C8}, DM_{C9}, and DM_{C10}), where these diamines act as permeant blockers (Guo and Lu, 2000).

Channel Block by Intracellular Polyamines

Fig. 7 A shows the current traces recorded between −100 and +100 mV in the absence or presence of various concentrations of the triamine spermidine. Practi-

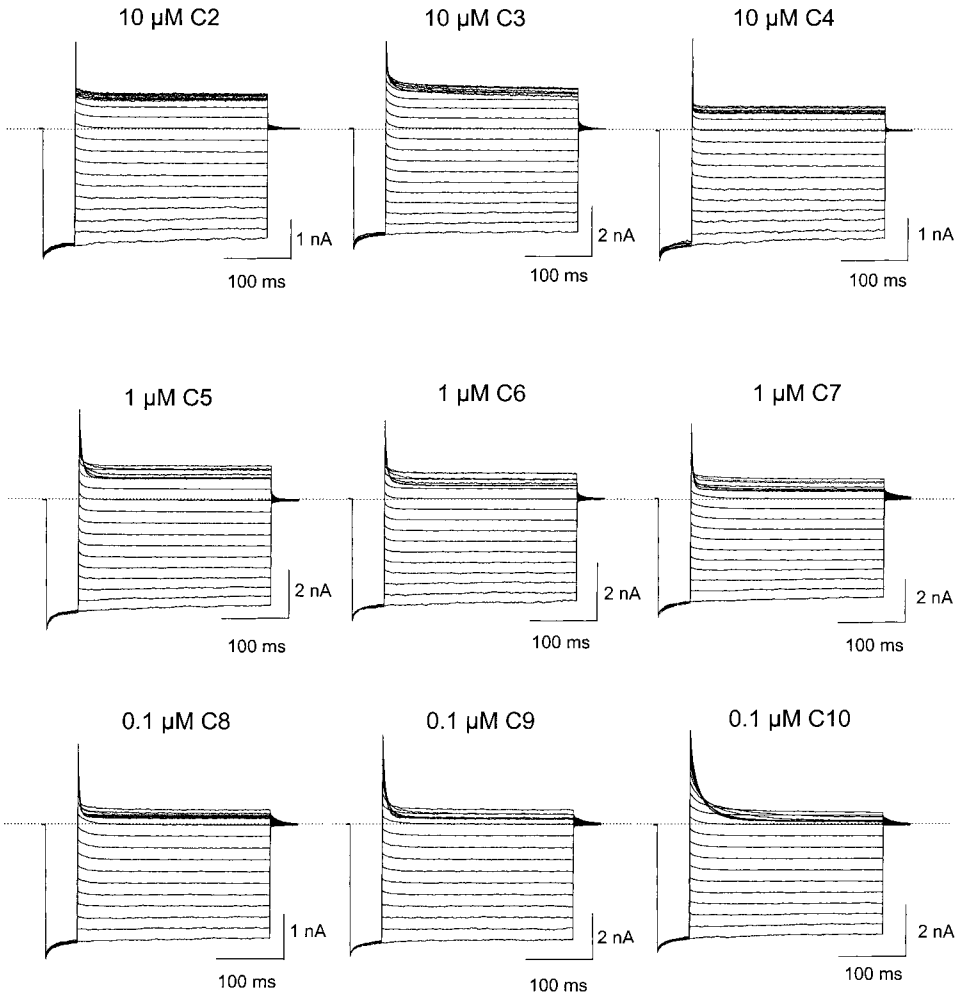

Figure 4. Channel block by a series of intracellular diamines. Current traces recorded in the presence of nine diamines (DM_{C2} through DM_{C10}, labeled as C2 through C10) at the concentration indicated. The voltage protocol was as for Fig. 3.

cally, 30 nM is the lowest concentration of spermidine at which the outward IRK1 current reaches a steady state within 300 ms after a voltage step. In Fig. 7 B, we plotted I-V curves recorded in the absence or presence of spermidine at three concentrations. The I-V curve in the presence of spermidine consists of multiple phases. Fig. 7 C shows the fractions of unblocked current at the three spermidine concentrations as a function of membrane voltage. As with diamines, the extent of channel block by spermidine tends to nonzero levels at positive membrane voltages, but a noticeable hump appears in spermidine-blocking curves that was absent from those of diamines.

Fig. 8 A shows channel block by the intracellular tetramine spermine. Although spermine appears to block the channel more effectively, it displays a complex blocking behavior generally similar to that of spermidine. The I-V curves in the presence of spermine also consist of multiple phases (Fig. 8 B). The spermine-blocking curves also have a hump, albeit less prominent than in the case of spermidine, preceding the plateau phase at positive voltages (Fig. 8 C). Over a comparable voltage range, the IRK1 channel blocking curves for spermine and spermidine shown here resemble somewhat those in the CNG channel (Guo and Lu, 2000), except that the humps are much less prominent in the IRK1 channel.

Channel Block by Spermidine at Two Different Intracellular pH

To test whether the multiphasic polyamine blocking curve is due to nonuniform protonation of the polyamine and/or the channel, we examined how intracellular pH affects channel block by spermidine. Fig. 9 A shows IRK1 channel current traces obtained at membrane voltages between −100 and +100 mV. The two sets of current traces Fig. 9 A, top, were recorded without and those below with intracellular spermidine. Fig. 9 A, left, were obtained at intracellular pH 7.6, those on the right at pH 6.6. As shown previously (Shieh et al., 1996), lowering intracellular pH from 7.6 to 6.6 reduced the outward current through the IRK1 channel at positive voltages. In Fig. 9 B, the fractions of unblocked current, obtained at intracellular pH 7.6 and 6.6, are plotted as a function of membrane voltage. Lowering pH from 7.6 to 6.6 results in noticeable, if

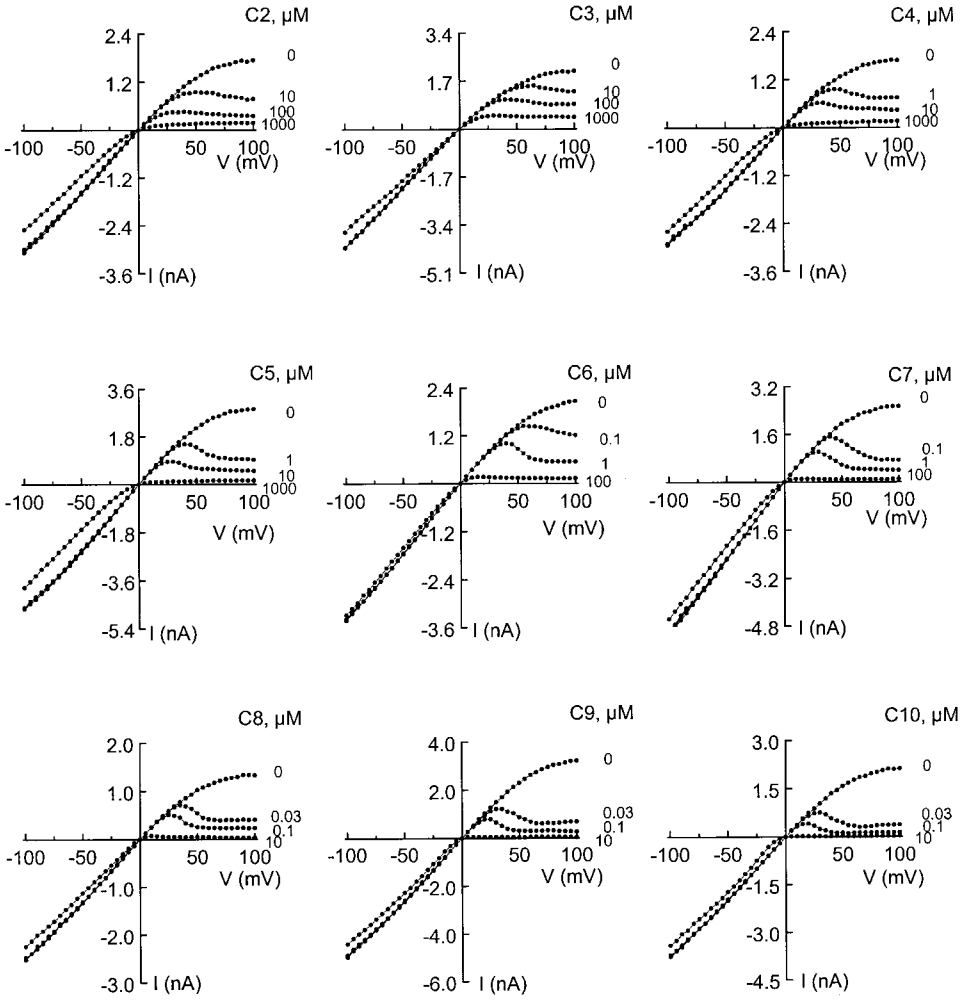

Figure 5. Effects of a series of intracellular diamines on the current–voltage relationship of the IRK1 channel. The I-V curves were obtained in the absence or presence of nine diamines (DM_{C2} through DM_{C10}, labeled C2 through C10) at the concentrations indicated.

small, changes in the spermidine-blocking curve: the hump decreases but the residual current at positive voltages increases.

Channel Block by a Spermine Derivative

To test whether the residual current at positive voltages is due to spermine being a permeant blocker, we examined block of the IRK1 channel by PhTx, essentially spermine with a bulky chemical group attached to one end. Fig. 10 A shows the current traces recorded at membrane voltages between −100 and +100 mV in the absence or presence of 10 μM PhTx. The corresponding I-V curves are shown in Fig. 10 B. In Fig. 10 C, we plotted the fractions of unblocked current as a function of membrane voltage. As in the case of TEA, the extent of channel block by PhTx increased monotonically with membrane voltage. Both the hump and the trailing "plateau" phase seen in the spermine-blocking curve are absent. The curve superimposed on the data points in Fig. 10 C is a fit of the Woodhull equation. Thus, PhTx blocks the IRK1 channel very much like a typical (nonpermeant) ionic pore blocker.

DISCUSSION

Block of the IRK1 channel by intracellular polyamines appears to be complex. To understand its mechanism, we examined channel blocking behaviors of di- and polyamines as a function of concentration and membrane voltage. Some of these blocking behaviors are reminiscent of those occurring in the CNG channel (Guo and Lu, 2000).

Channel Block by Diamines

As observed previously by Pearson and Nichols (1998), channel block by all primary diamines tested remains incomplete at positive membrane voltages (Fig. 6). To analyze the voltage dependence of channel block, Pearson and Nichols (1998) modified the Woodhull equation by adding a constant to account for the current remaining at positive voltages. The residual current is not likely to result from (a) diamine-induced discrete subconductance state(s) because we found that the amplitude of the residual current decreases when diamine concentration is raised (Fig. 6). We observed a similar phenome-

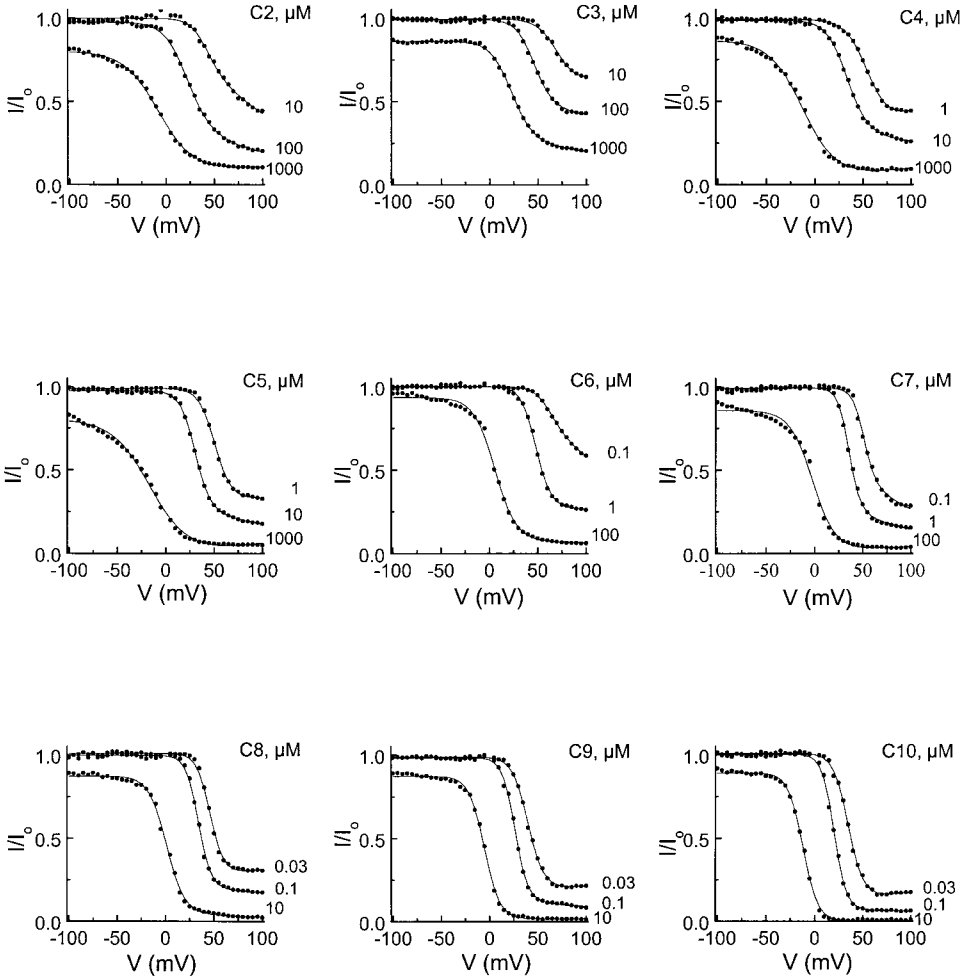

Figure 6. Voltage dependence of channel block by a series of intracellular diamines. The fractions of unblocked current in the presence of various diamines (DM_{C2} through DM_{C10}, labeled C2 through C10) at the indicated concentrations were plotted as a function of membrane voltage. The curves superimposed on the data are fits of Eq. 2. From each fit, the current at a given voltage was normalized to the value at −100 mV.

non in block of CNG channels by some longer diamines that appear to permeate very slowly through the channel (Guo and Lu, 2000). Thus, the persisting current observed here at very positive voltages likely results also from diamines being permeant blockers, as illustrated in Fig. 11 A, for which the fraction of unblocked channels and thus unblocked current is given by:

$$\frac{I}{I_o} = \frac{1}{1 + [DM]\left(\dfrac{k_1 e^{\frac{z_1 F V_m}{RT}}}{k_{-1} e^{\frac{-z_{-1} F V_m}{RT}} + k_{-2} e^{\frac{z_{-2} F V_m}{RT}}}\right)} \quad (1)$$

or

$$\frac{I}{I_o} = \frac{1}{1 + \dfrac{[DM]}{\left(1 + \dfrac{k_{-2}}{k_{-1}} e^{\frac{(z_{-1} + z_{-2}) F V_m}{RT}}\right) K_1 e^{\frac{-Z_1 F V_m}{RT}}}}, \quad (2)$$

where [DM] is the intracellular diamine concentration (the extracellular diamine concentration is zero) and all rate constants are assumed to vary exponentially with membrane voltage. The four independent parameters are: K_1, the equilibrium dissociation constant for channel-diamine interaction; k_{-2}/k_{-1}, the relative probability of a diamine bound in the pore permeating the pore versus returning to the intracellular solution; and the corresponding apparent valences Z_1 and "$z_{-1} + z_{-2}$". The curves superimposed on the data in Fig. 6 are fits of Eq. 2.

Values for these four adjustable parameters, determined from the fits, are plotted against diamine methylene chain length in Fig. 12. The value of K_1 generally decreases with increasing methylene chain length (Fig. 12 A), consistent with the observation that longer diamines are more potent blockers (Fig. 5). Thus, as previously suggested (Pearson and Nichols, 1998), hydrophobic interactions are critical in mediating interactions between diamines and the pore.

Fig. 12 C shows that k_{-2}/k_{-1} is rather small and decreases (from 0.05 to 0.01) with increasing methylene chain length. Since k_{-2}/k_{-1} is the relative probability of a molecule bound in the pore traversing the pore versus returning to the intracellular solution, the result shows that diamines traverse the pore very infrequently.

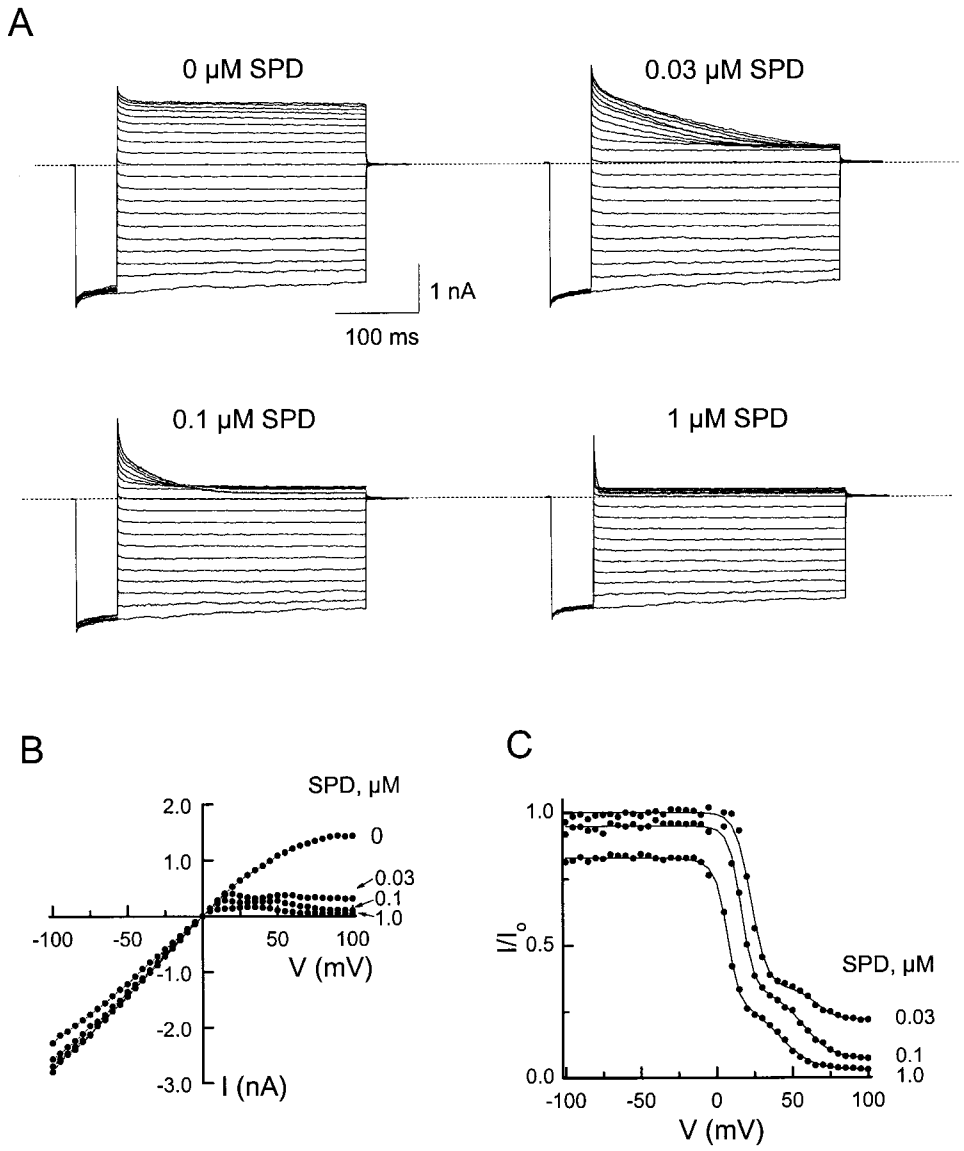

Figure 7. Channel block by intracellular spermidine. (A) Current traces recorded in the absence or presence of various concentrations of spermidine. The voltage protocol was as for Fig. 3. (B) I-V curves in the absence or presence of various concentrations of spermidine. (C) The fractions of current not blocked by spermidine are plotted as a function of membrane voltage. The curves are fits of Eq. 6. For each fit, the current at a given voltage was normalized to the value at −100 mV. The parameters determined from the fits are: $K^a_1 = 6.7$ (± 0.6) $\times 10^{-6}$ M, $Z^a_1 = 5.0 \pm 0.1$; $k^a_{-2}/k^a_{-1} = 3.2$ (± 0.7) $\times 10^{-2}$, "$z^a_{-1} + z^a_{-2}$" $= 5.1 \pm 0.1$; $K^b_1 = 2.9$ (± 0.3) $\times 10^{-5}$ M, $Z^b_1 = 3.2 \pm 0.1$; $k^b_{-2}/k^b_{-1} = 3.0$ (± 0.6) $\times 10^{-3}$, "$z^b_{-1} + z^b_{-2}$" $= 3.4 \pm 0.1$ (mean $\pm$ SEM, $n = 9$).

However, a few percent of bound diamine molecules popping through the pore allow sufficient K^+ permeation to account for the residual current at positive membrane voltages. Furthermore, k_{-2}/k_{-1} decreases with increasing methylene chain length, consistent with the expectation that more hydrophobic diamines are less likely to traverse the pore.

The valence factors Z_1 and "$z_{-1} + z_{-2}$" also increase with methylene chain length (Fig. 12, B and D). Empirically, Z_1 and "$z_{-1} + z_{-2}$" for a given diamine appear to be numerically similar. If, for the sake of discussion, one assumes that for a given diamine, quantities Z_1 and "$z_{-1} + z_{-2}$" are equal, then Eq. 1 simplifies to:

$$\frac{I}{I_o} = \frac{1}{1 + \dfrac{[DM]}{K_1 e^{\frac{-Z_1 F V_m}{RT}} + \dfrac{k_{-2}}{k_1}}}. \quad (3)$$

At a sufficiently high membrane voltage, Eq. 3 approaches a voltage-independent constant value determined solely by diamine concentration:

$$\frac{I}{I_o} = \frac{1}{1 + \dfrac{k_1}{k_{-2}}[DM]}, \quad (4)$$

which explains why at a given diamine concentration the voltage-dependent inhibition curve can be well fitted using the Woodhull equation, provided an extra constant is included to represent residual current at positive membrane voltages (Pearson and Nichols, 1998).

Eq. 4 can be appreciated in an intuitive way. When a lodged diamine molecule pops through the pore, a brief window of opportunity is created for K^+ ions to "leak" through the pore; the window closes when another diamine molecule becomes lodged in the pore.

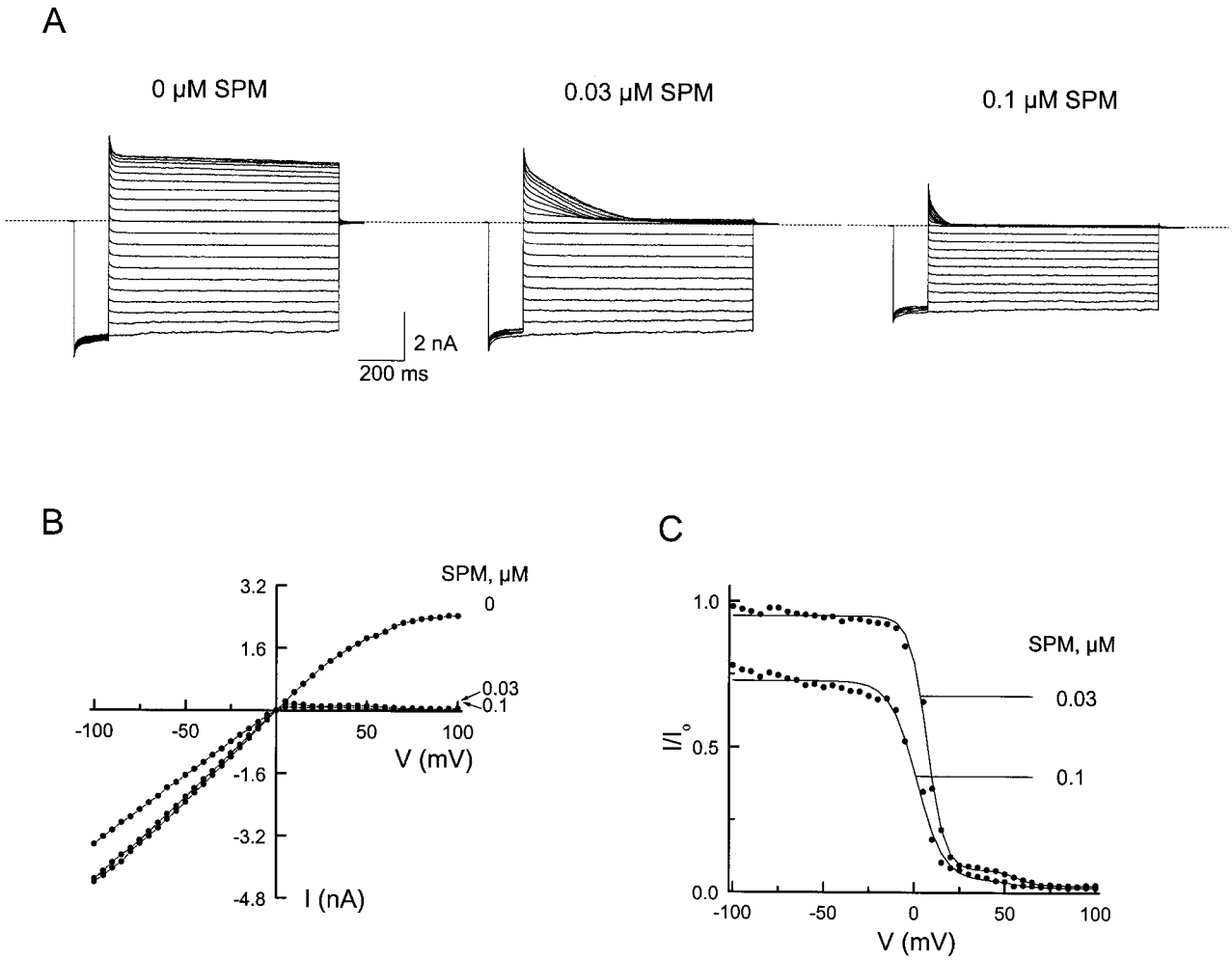

Figure 8. Channel block by intracellular spermine. (A) Current traces recorded in the absence or presence of two concentrations of spermine. The voltage protocol was as for Fig. 3, except that the voltage pulses were 1-s long. (B) I-V curves in the absence or presence of the two concentrations of spermine. (C) The fractions of current not blocked by spermine are plotted against membrane voltage. The curves superimposed on the data are fits of Eq. 6. For each fit, the current at a given voltage was normalized to the value at −100 mV. The parameters determined from the fits are: $K^a_1 = 2.3\ (\pm 0.5) \times 10^{-7}$ M, $Z^a_1 = 5.4 \pm 0.2$; $k^a_{-2}/k^a_{-1} = 2.8\ (\pm 0.8) \times 10^{-2}$, "$z^a_{-1} + z^a_{-2}$" $= 5.6 \pm 0.3$; $K^b_1 = 4.6\ (\pm 0.7) \times 10^{-6}$ M, $Z^b_1 = 3.7 \pm 0.3$; $k^b_{-2}/k^b_{-1} = 8.5\ (\pm 0.9) \times 10^{-4}$, "$z^b_{-1} + z^b_{-2}$" $= 3.9 \pm 0.2$ (mean ± SEM, $n = 9$).

Either a higher diamine binding rate (k_1[DM]) or a lower rate of bound diamine popping through the pore (k_{-2}), or both, will reduce the time available for K^+ to leak and thus leave a smaller residual current. This explains why the residual current is inversely related to diamine concentration (Fig. 6). Although diamines may permeate the channel, their intrinsic rate of permeation is too slow to account for the residual current. Nearly all the observed residual current must be carried by K^+ ions because it vanishes at sufficiently high blocker concentrations (Fig. 6).

Channel Block by Polyamines

Fig. 7 C shows the voltage-dependent blocking curve of the IRK1 channel in the presence of three concentrations of the triamine spermidine. Above 0 mV, the curve descends rapidly as membrane voltage is increased, and it then forms a hump before approaching a nonzero level at extreme positive voltages. Clearly, the curve cannot be fitted by a Woodhull equation. These blocking curves are reminiscent of those of the CNG channel in the presence of intracellular polyamines, although the hump observed here is much less prominent (Guo and Lu, 2000). To account for the multiphasic spermidine-blocking curve, we used a model, shown in Fig. 11 B, which assumes that binding of spermidine to the channel can lead to two blocked states. In each of the two blocked states, spermidine is bound with different affinity and has a different probability of traversing the pore. Interconvertibility between the two blocked states cannot be assessed based on the steady

state data presented here. For simplicity, our model assumes no direct transition between the two blocked states. The fraction of unblocked channel and thus unblocked current is given by Eq. 5:

$$\frac{I}{I_o} = \frac{1}{1+[PM]} \cdot \frac{1}{\left(\frac{k_1^a e^{\frac{z_1^a F V_m}{RT}}}{k_{-1}^a e^{\frac{-z_{-1}^a F V_m}{RT}} + k_{-2}^a e^{\frac{z_{-2}^a F V_m}{RT}}} + \frac{k_1^b e^{\frac{z_1^b F V_m}{RT}}}{k_{-1}^b e^{\frac{-z_{-1}^b F V_m}{RT}} + k_{-2}^b e^{\frac{z_{-2}^b F V_m}{RT}}} \right)} \quad (5)$$

or, upon rearranging:

$$\frac{I}{I_o} = 1 \Big/ \left\{ 1 + \left[\frac{[PM]}{\left(1 + \frac{k_{-2}^a}{k_{-1}^a} e^{\frac{(z_{-1}^a + z_{-2}^a) F V_m}{RT}} \right) K_1^a e^{\frac{-Z_1^a F V_m}{RT}}} + \frac{[PM]}{\left(1 + \frac{k_{-2}^b}{k_{-1}^b} e^{\frac{(z_{-1}^b + z_{-2}^b) F V_m}{RT}} \right) K_1^b e^{\frac{-Z_1^b F V_m}{RT}}} \right] \right\}, \quad (6)$$

where [PM] is the intracellular polyamine concentration (the extracellular polyamine concentration is zero) and all rate constants are assumed to vary exponentially with membrane voltage. As shown in Fig. 7, the spermidine-blocking curves can be well fitted by Eq. 6.

Since the IRK1 channel is inhibited by intracellular protons, and polyamines are not fully protonated near neutral pH (Palmer and Powell, 1974), we wonder whether the different blocked channel states result from nonuniform protonation of either the polyamines or the channel. Therefore, we examined how altering intracellular pH affects the spermidine-blocking curve. Lowering intracellular pH from 7.6 to 6.6 reduces the hump in the curve, but enhances the residual current at positive voltages (Fig. 9 B). Consequently, the blocking curves for the two pH values cross, a phenomenon qualitatively similar to that seen with spermine in the CNG channel. To analyze the data, we used a model that assumes that the two blocked states result from nonuniform protonation of a site in spermidine (or in the channel) (Guo and Lu, 2000). According to the model:

$$\frac{I}{I_o} = 1 \Big/ \left\{ 1 + [PM] \left[\frac{\theta}{\left(1 + \frac{k_{-2}^a}{k_{-1}^a} e^{\frac{(z_{-1}^a + z_{-2}^a) F V_m}{RT}} \right) K_1^a e^{\frac{-Z_1^a F V_m}{RT}}} + \frac{1-\theta}{\left(1 + \frac{k_{-2}^b}{k_{-1}^b} e^{\frac{(z_{-1}^b + z_{-2}^b) F V_m}{RT}} \right) K_1^b e^{\frac{-Z_1^b F V_m}{RT}}} \right] \right\}, \quad (7)$$

where $\Theta = 10^{-pH}/(10^{-pH} + 10^{-pKa})$. The smooth traces superimposed on the blocking curves in Fig. 9 B are simultaneous fits of Eq. 7 to the two curves. From the fit, we deduced a pKa for the titrated site of 8.1 ± 0.1 (mean ± SEM). Given this value, much larger changes in the blocking curve should be observed if the intracellular pH were raised from 7.6 rather than lowered. Unfortunately, channel currents run down very rapidly above pH 8.0.

Palmer and Powell (1974) determined the three pKa values of spermidine as 10.9, 9.8, and 8.3 (100 mM ionic strength and 25°C), the latter comparable to the value of 8.1 that we find for the titratable site influencing spermidine block. If the titratable site is indeed an amine group in spermidine, then the fully protonated spermidine should correspond to the higher affinity and more permeant conformation, while the partially protonated molecule corresponds to the lower affinity and less permeant component. These inferences are compatible with the observation that the apparent valence of the high-affinity blocking component is larger than that of the low affinity one. However, the absolute value of the valence factor undoubtedly does not solely reflect the charges on spermidine, because the valence value associated with the high-affinity blocking component is ~5. Although, unlike TEA or Mg^{2+} (Spassova and Lu, 1998), polyamines such as spermidine and spermine may bind in the narrow region of the pore where most of the voltage drop occurs, the movement of a polyamine molecule alone within the electrical field obviously cannot account for an observed valence of ~5. Therefore, the rather large valence values associated with channel block by polyamines (and diamines) most likely reflect a concerted movement of both the blocking ion and K^+ ions residing in the pore, as shown for block of the ROMK1 channel by TEA and Mg^{2+} (Spassova and Lu, 1998, 1999).

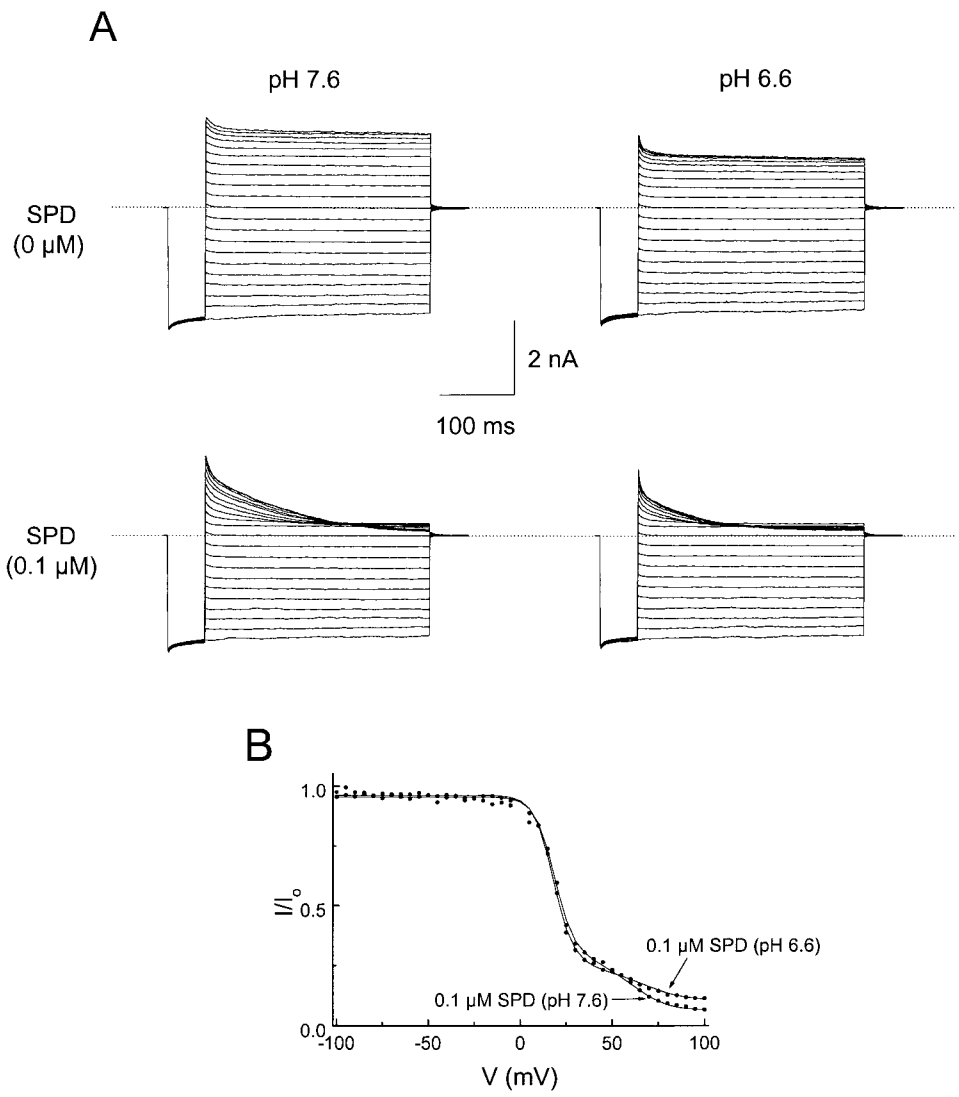

Figure 9. Intracellular pH dependence of IRK1 channel block by intracellular spermidine. (A) Families of current traces at various membrane voltages from −100 to +100 mV. The two sets of current traces (top and bottom) were obtained without and with spermidine, respectively. The two sets of current traces (left and right) were obtained at intracellular pH 7.6 and 6.6, respectively. Extracellular pH was 7.6 in both cases. The voltage protocol was as for Fig. 3. (B) The fractions of unblocked current in the presence of 0.1 μM spermidine at intracellular pH 6.6 and 7.6 are plotted as a function of membrane voltage. The smooth curves were obtained by simultaneously fitting Eq. 7 to the two data curves. The values of all parameters obtained from the fit are: K^a_1 = 3.7 (±0.4) × 10^{-6} M, Z^a_1 = 5.0 ± 0.2; k^a_{-2}/k^a_{-1} = 2.0 (±0.3) × 10^{-2}, "$z^a_{-1} + z^a_{-2}$" = 4.8 ± 0.1; K^b_1 = 5.0 (±0.1) × 10^{-5} M, Z^b_1 = 3.3 ± 0.2; k^b_{-2}/k^b_{-1} = 4.1 (± 1.0) × 10^{-3}, "$z^b_{-1} + z^b_{-2}$" = 3.3 ± 0.1; and pKa = 8.1 ± 0.1 (mean ± SEM, n = 3).

Intracellular protonation inhibits the IRK1 channel and also affects its gating, presumably by titrating a site in the channel with apparent pKa = 6.2 (Shieh et al., 1996), rendering the channel population also nonhomogeneous near neutral pH. Therefore, despite the fact that the multiphasic blocking curve can be well accounted for by a model in which spermidine exists in two protonated states with different affinities and permeabilities, we wish to emphasize that, in principle, the different blocking states may also in part result from nonhomogeneity of the channel.

As shown in Fig. 8 C, the blocking behavior of the tetramine spermine is very similar to that of the triamine spermidine and can be accounted for by the same model. However, the blocking behavior of a spermine derivative, PhTx, is quite different—no significant residual current was observed at positive voltages when the channel was blocked by PhTx (Fig. 10), as in the glutamate- and cGMP-gated channels (Bähring et al., 1997; Guo and Lu, 2000). It is as if the bulky group attached to the end of spermine effectively prevents the molecule from sliding through the channel. Compared with spermine, PhTx has a much lower affinity and apparent valence, consistent with a scenario where the bulky group hinders the interaction between spermine and the channel. A much lower affinity of the channel for a similar toxin, PhTx 433, than for spermine has also been observed by Lee et al. (1999). As shown in Fig. 10 C, the voltage-dependent block by PhTx is well described by the Woodhull equation. These findings support the idea that polyamines are permeant blockers in the IRK1 channel. Although the current is nearly voltage independent at negative potentials for a given concentration of PhTx, as well as di- and polyamines, it decreases when their concentration is increased. Thus, these polyamines must also inhibit the channel in a voltage-independent manner; e.g, by polyamine binding at the innermost part of the pore, where no signifi-

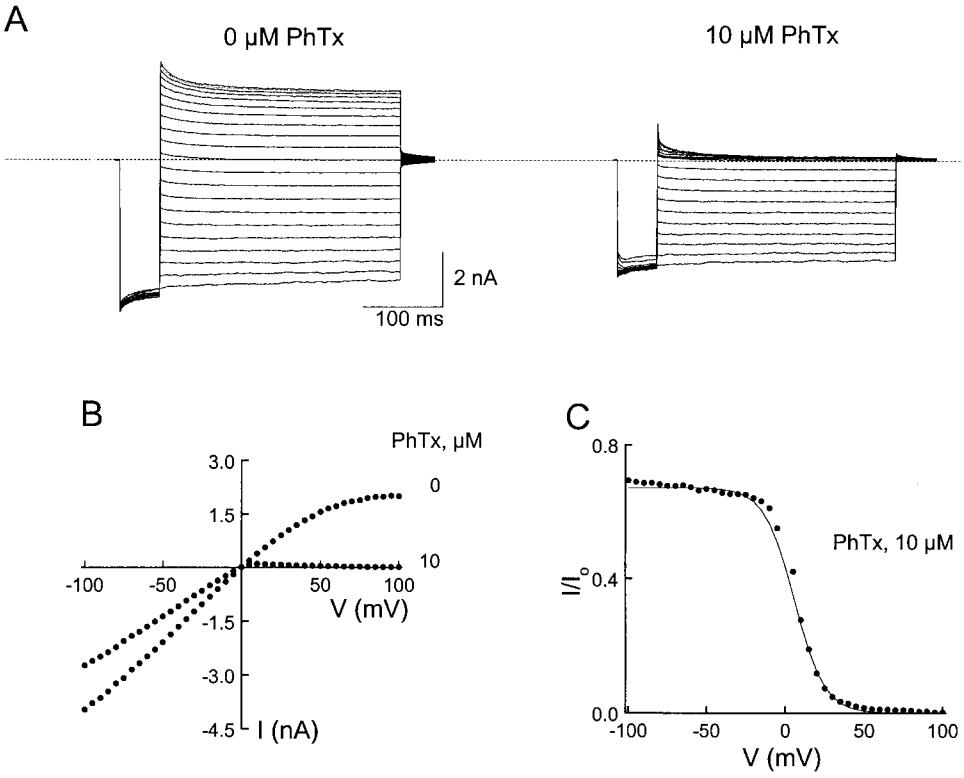

Figure 10. Channel block by intracellular PhTx. (A) Current traces recorded in the absence or presence of 10 μM PhTx. The voltage protocol was as for Fig. 3. (B) I-V curves in the absence or presence of 10 μM PhTx. (C) The fraction of current not blocked by 10 μM PhTx is plotted against membrane voltage. The curve is a fit of the Woodhull equation, $I/I_o = 1/(1 + [\mathrm{PhTx}]/K_d e^{-ZFV/RT})$. During the fit, the current at a given voltage was normalized to the value at −100 mV. The values of K_d and Z determined from the fits are 21.3 ± 0.4 μM and 2.8 ± 0.1 (mean ± SEM, $n = 3$), respectively.

cant voltage drop occurs, or by a mechanism that does not involve the pore.

As in the case of diamines, comparable Z_1 and "$z_{-1} + z_{-2}$" values for each state (*a* and *b*) are needed to fit the polyamine-blocking curves. For the purpose of illustration, if one assumes Z^a_1 and "$z^a_{-1} + z^a_{-2}$" to be numerically equal (denoted Z^a) and Z^b_1 and "$z^b_{-1} + z^b_{-2}$" to be numerically equal (denoted Z^b), then Eq. 6 becomes Eq. 8:

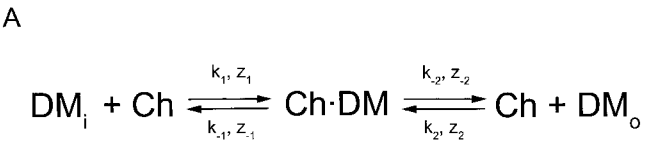

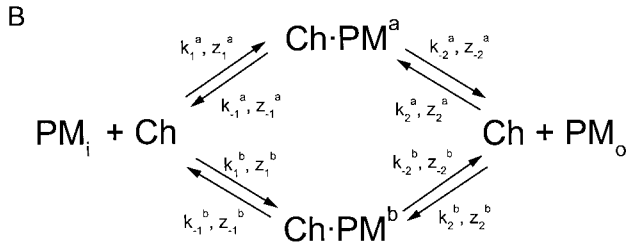

Figure 11. Kinetic schemes for channel block by di- and polyamines. A assumes that a diamine (DM) blocks the channel (Ch) as a permeant blocker. B assumes that a polyamine (PM) blocks the channel (Ch) in two possible conformations, a and b. Parameters k_x and z_x are the rate constant and apparent valence, respectively, for a given transition.

$$\frac{I}{I_o} = \frac{1}{1 + \dfrac{[\mathrm{PM}]}{\left(1 + \dfrac{k^a_{-2}}{k^a_{-1}} e^{\frac{Z^a F V_m}{RT}}\right) K^a_1 e^{\frac{-Z^a F V_m}{RT}} + \left(1 + \dfrac{k^b_{-2}}{k^b_{-1}} e^{\frac{Z^b F V_m}{RT}}\right) K^b_1 e^{\frac{-Z^b F V_m}{RT}}}} \tag{8}$$

or, upon rearranging:

$$\frac{I}{I_o} = \frac{1}{1 + \dfrac{1}{\dfrac{K^a_1 e^{\frac{-Z^a F V_m}{RT}} + K^b_1 e^{\frac{-Z^b F V_m}{RT}}}{[\mathrm{PM}]} + \dfrac{\dfrac{k^a_{-2}}{k^a_1} + \dfrac{k^b_{-2}}{k^b_1}}{[\mathrm{PM}]}}}. \tag{9}$$

Furthermore, for spermidine concentrations much greater than the sum of k^a_{-2}/k^a_1 and k^b_{-2}/k^b_1, Eq. 9 approaches Eq. 10:

$$\frac{I}{I_o} = \frac{1}{1 + \dfrac{[\mathrm{PM}]}{K^a_1 e^{\frac{-Z^a F V_m}{RT}} + K^b_1 e^{\frac{-Z^b F V_m}{RT}}}}, \tag{10}$$

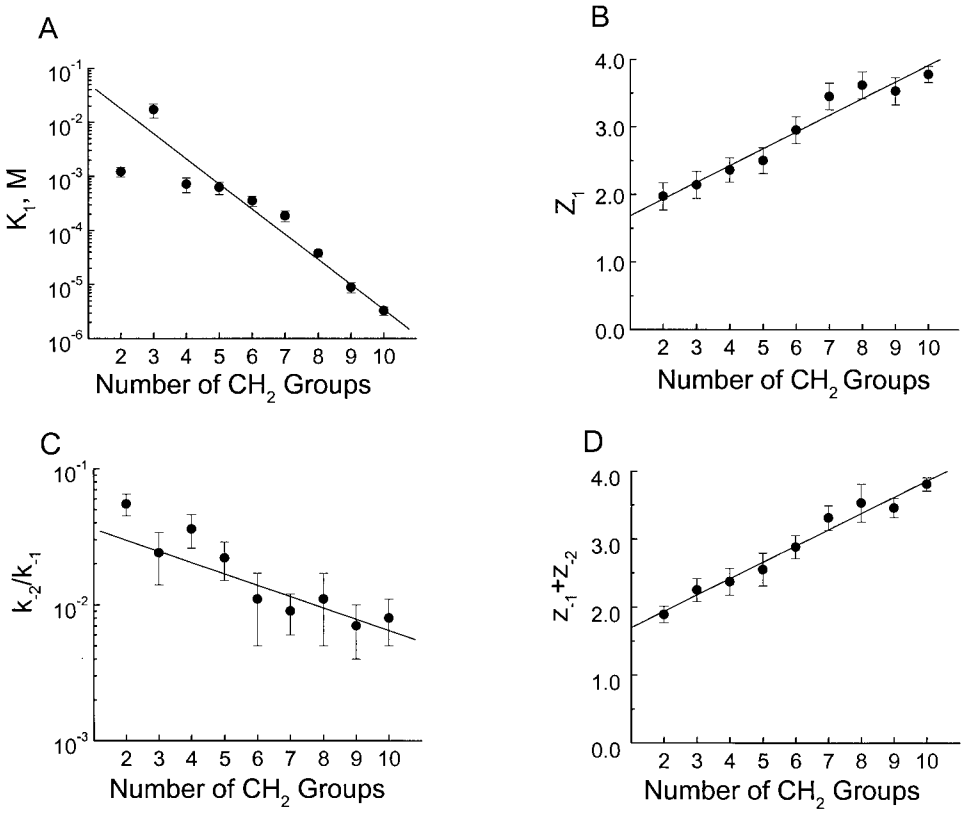

Figure 12. Analysis of channel block by primary diamines of varying methylene chain length. Parameters K_1, Z_1, k_{-2}/k_{-1}, and "$z_{-1} + z_{-2}$" (mean ± SEM, $n = 9$) are plotted in A–D against the number of methylene groups in each diamine. The parameters were obtained by fitting Eq. 2 to the data, as shown in Fig. 6.

showing that the voltage dependence of channel block by polyamines at high concentrations can be approximated by an equation with two Boltzmann terms (compare Lopatin et al., 1995). When $K_1^a << K_1^b$ and also $Z_1^a > Z_1^b$, at some positive voltages, Eq. 9 approximates:

$$\frac{I}{I_o} = \frac{1}{1 + \dfrac{[PM]}{K_1^b e^{\frac{-Z^b F V_m}{RT}} + \dfrac{k_{-2}^a}{k_1^a} + \dfrac{k_{-2}^b}{k_1^b}}}, \quad (11)$$

producing a hump (Fig. 7 C). At extreme positive voltages, Eq. 11 approaches Eq. 12:

$$\frac{I}{I_o} = \frac{1}{1 + \dfrac{[PM]}{\dfrac{k_{-2}^a}{k_1^a} + \dfrac{k_{-2}^b}{k_1^b}}}, \quad (12)$$

accounting for the residual current at these voltages. As in the case of diamines, the amplitude of the residual current should decrease with increasing spermidine concentration and tend towards zero at very high concentrations, as observed (Fig. 7 C).

Currents through the IRK1 channel after a jump to positive membrane voltages decline with time even in patches exhaustively perfused with nominally blocking ion-free solution. It has been suggested that this decline in current results from intrinsic gating (Aleksandrov et al., 1996; Shieh et al., 1996; Lee et al., 1999), although both the extent and the rate of the current decline appear to vary considerably among various reported studies. Here, we found that the voltage dependence of the current decline is much weaker than that of block by high-affinity endogenous polyamines spermine and spermidine. This finding argues that the current decline reflects either the hypothesized intrinsic gating or channel block by some contaminating blockers other than spermine or spermidine. For presentation purposes, we will adopt the current nomenclature "intrinsic gating" when referring to the voltage-dependent current decline. The hypothesized intrinsic gating will complicate our analysis somewhat, but will not fundamentally affect our conclusions. The hump in the spermidine (or spermine)-blocking curve occurs between +20 and +50 mV, where the current decline due to intrinsic gating is minimal (Fig. 1). To include intrinsic gating (or channel block by contaminating blocking ions), at least one more non- or subconducting state (Ch*) is required (Fig. 13). For simplicity, we treat Ch* here as a nonconducting state. In principle, channels in the Ch* state may or may not be occupied by a polyamine, and channels in Ch state occupied by a polyamine may or may not undergo the gating transition. Additional non–steady state experiments are needed to evaluate these possibilities. According to Fig. 13, the reciprocals of both equilibrium constants in steady state Eq. 7 need to be multiplied by a term, as indicated by Eq. 13:

$$\frac{I}{I_o} = \frac{1}{1 + [PM]\left[\frac{\theta}{\left(1 + \frac{k^a_{-2}}{k^a_{-1}} e^{\frac{(z^a_{-1} + z^a_{-2})F V_m}{RT}}\right) K^a_1 e^{\frac{-Z^a_1 F V_m}{RT}}} + \frac{1 - \theta}{\left(1 + \frac{k^b_{-2}}{k^b_{-1}} e^{\frac{(z^b_{-1} + z^b_{-2})F V_m}{RT}}\right) K^b_1 e^{\frac{-Z^b_1 F V_m}{RT}}}\right]\left(\frac{1}{1 + K^* e^{\frac{-Z^* F V_m}{RT}}}\right)}, \quad (13)$$

where K* is [Ch*]/[Ch], and Z* is the associated valence factor. Under our experimental conditions, the fitted values for both K* (0.03 ± 0.01; mean ± SEM) and Z* (0.55 ± 0.01) are small (Fig. 1 C), yielding multiplier values that range from 0.97 at 0 mV to 0.80 at +100 mV. Therefore, the addition of this nonconducting state would cause only minor changes in the fitted equilibrium constants (K_1^a and K_1^b) and valence factors (Z_1^a and Z_1^b), but has no fundamental impact on our analysis.

Models involving channel gating have previously been proposed to explain various aspects of intracellular cation-induced inward rectification in the IRK1 channel. For example, Aleksandrov et al. (1996) proposed that intracellular Mg^{2+} and polyamines inhibit the channel by controlling a gate located at its intracellular end. Subsequently, Lee et al. (1999) proposed a more detailed physical model where one end of the polyamine molecule is tethered to a channel gate while the other plugs the pore. The spermine-gate complex is assumed to block the channel with high affinity, while spermine itself has only low affinity. Kinetically, both their model and our model have one conducting and three nonconducting states, including the nonconducting gating state. However, the four-state model of Lee et al. (1999), without additional features, predicts that the current in the presence of polyamine will decrease with increasing membrane voltage in multiexponential fashion and eventually vanish. In other words, their model accounts for neither the hump nor the residual current at positive voltages that we observed in the polyamine-blocking curve, because it lacks a voltage-dependent mechanism that opposes the current reduction due to channel gating or block. To account for these unusual characteristics, our model invokes two essential features: in the two blocked states, the polyamine molecules are bound not only with different affinities, but also, more critically, with different probabilities of traversing the pore. The K^+ leak currents resulting from the finite polyamine permeabilities can fully account for both the hump and the residual current at positive voltages. Our proposal is supported by the absence of significant humps or residual currents at positive voltages in the curves of the bulky blocker PhTx or of TEA.

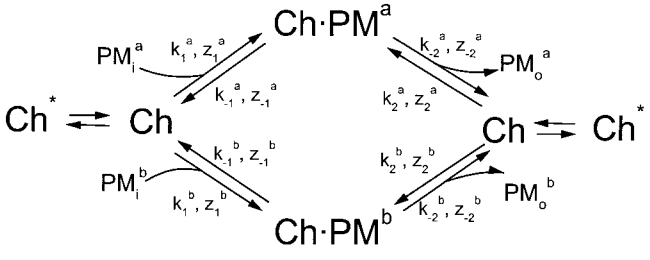

Figure 13. A kinetic model that includes an additional nonconducting state. To include the intrinsic gating (or channel block by contaminating blocking ions), an additional nonconducting state (Ch*) is incorporated into the scheme of Fig. 11 B. K* = [Ch*]/[Ch] is the equilibrium constant of the transition between Ch and Ch*, while Z* is the associated valence.

We thank L.Y. Jan for the IRK1 channel cDNA clone, P. De Weer for critical review and discussion of our manuscript, and C.M. Armstrong, C. Deutsch, and G. Yellen for helpful discussions.

This study was supported by National Institutes of Health (NIH) grant GM55560. Z. Lu was a recipient of an Independent Scientist Award from NIH (HL03814).

Submitted: 19 August 1999
Revised: 8 May 2000
Accepted: 11 May 2000

REFERENCES

Aleksandrov, A., B. Velimirovic, and D.E. Clapham. 1996. Inward rectification of the IRK1 K^+ channel reconstituted in lipid bilayers. *Biophys. J.* 70:2680–2687.

Armstrong, C.M., and L. Binstock. 1965. Anomalous rectification in the squid giant axon injected with tetraethylammonium. *J. Gen. Physiol.* 48:859–872.

Bähring, R., D. Bowie, M. Benveniste, and M.L. Mayer. 1997. Permeation and block of the rat GluR6 glutamate receptor channels by internal and external polyamines. *J. Physiol.* 502:575–589.

Fakler, B., U. Brandle, E. Glowatzki, S. Weidemann, H.P. Zenner, and J.P. Ruppersburg. 1995. Strong voltage-dependent inward-rectification of inward-rectifier K^+ channels is caused by intracellular spermine. *Cell.* 80:149–154.

Ficker, E., M. Taglialatela, B.A. Wible, C.M. Henley, and A.M. Brown. 1994. Spermine and spermidine as gating molecules for inward rectifier K^+ channels. *Science.* 266:1068–1072.

Guo, D., and Z. Lu. 2000. Mechanism of cGMP-gated channel block by intracellular polyamines. *J. Gen. Physiol.* 115:783–797.

Hille, B. 1992. Ionic Channels of Excitable Membranes. 2nd ed. Sinauer Associates, Inc., Sunderland, MA. 607 pp.

Horie, M., H. Irisawa, and H. Noma. 1987. Voltage-dependent magnesium block of adenosine- triphosphate–sensitive potassium channel in guinea-pig ventricular cells. *J. Physiol.* 387:251–272.

Kubo, Y., T.J. Baldwin, Y.N. Jan, and L.Y. Jan. 1993. Primary structure and functional expression of a mouse inward rectifier potassium channel. *Nature.* 362:127–133.

Lee, J.-K., J.A. Scott, and J.N. Weiss. 1999. Novel gating mechanism of polyamine block in the strong inward rectifier K channel Kir2.1. *J. Gen. Physiol.* 113:555–563.

Logothetis, D.E., Y. Kurachi, J. Galper, E.J. Neer, and D.E. Clapham. 1987. The βγ subunits of GTP-binding proteins activate the muscarinic K^+ channel in heart. *Nature.* 325:321–326.

Lopatin, A.N., E.N. Makhina, and C.G. Nichols. 1994. Potassium channel block by cytoplasmic polyamines as the mechanism of intrinsic rectification. *Nature.* 372:366–369.

Lopatin, A.N., E.N. Makhina, and C.G. Nichols. 1995. The mechanism of inward rectification of potassium channels: "long-pore plugging" by cytoplasmic polyamines. *J. Gen. Physiol.* 106:923–955.

Lu, T., B. Nguyen, X. Zhang, and J. Yang. 1999. Architecture of a K^+ channel inner pore revealed by stoichiometric covalent modification. *Neuron.* 22:571–580.

Lu, Z., and R. MacKinnon. 1994. Electrostatic tuning of Mg^{2+} affinity in an inward-rectifier K^+ channel. *Nature.* 371:243–246.

Matsuda, H., A. Saigusa, and H. Irisawa. 1987. Ohmic conductance through the inward-rectifier K^+ channel and blocking by internal Mg^{2+}. *Nature.* 325:156–159.

Oliver, D., H. Hahn, C. Antz, J.P. Ruppersberg, and B. Fakler. 1998. Interaction of permeant and blocking ions in cloned inward-rectifier K^+ channels. *Biophys. J.* 74:2318–2326.

Pearson, W.L., and C.G. Nichols. 1998. Block of the Kir2.1 channel pore by alkylamine analogues of endogenous polyamines. *J. Gen. Physiol.* 112:351–363.

Palmer, B.N., and H.K.J. Powell. 1974. Polyamine complex with seven-membered chelate rings: complex formation of 3-azaheptane-1,7-diamine, 4-azaoctane-1,8-diamine (spermidine), and 4,9-diazadodecane-1,12-diamine (spermine) with copper (II) and hydrogen ions in aqueous solution. *J. Chem. Soc. Dalton Trans.* 19: 2089–2092.

Shieh, R.C., S.A. John, J.-K. Lee, and J.N. Weiss. 1996. Inward rectification of IRK1 expressed in *Xenopus* oocytes: effects of intracellular pH reveal an intrinsic gating mechanism. *J. Physiol.* 494: 363–376.

Spassova, M., and Z. Lu 1998. Coupled ion movement underlies rectification in an inward-rectifier K^+ channel. *J. Gen. Physiol.* 112:211–221.

Spassova, M., and Z. Lu 1999. Tuning the voltage dependence of tetraethylammonium block with permeant ions in an inward-rectifier K^+ channel. *J. Gen. Physiol.* 114:415–426.

Vandenberg, C.A. 1987. Inward rectification of a potassium channel in cardiac ventricular cells depends on internal magnesium ions. *Proc. Natl. Acad. Sci. USA.* 84:2560–2564.

Woodhull, A.M. 1973. Ionic blockage of sodium channels in nerve. *J. Gen. Physiol.* 61:687–708.

Yang, J., Y.N. Jan, and L.Y. Jan. 1995. Control of rectification and permeation by residues in two distinct domains in an inward rectifier K^+ channel. *Neuron.* 14:1047–1054.